[56]J. Singer, J. Phys. Chem. Solids 24, 1645 (1963).
[57]E. Steigmeier, in *Thermal Conductivity*, edited by R. P. Tye (Academic, New York, 1969), Vol. 2, Chap. 4.
[58]G. Leibfried and E. Schlömann, Nachr. Akad. Wiss. Göttingen, II. Math. Phys. Klasse 4, 71 (1954).
[59]G. A. Slack, J. Phys. Chem. Solids (to be published).
[60]C. F. Cline, H. L. Dunegan, and G. W. Henderson, J. Appl. Phys. 38, 1944 (1967).
[61]R. A. Robie and J. L. Edwards, J. Appl. Phys. 37, 2659 (1966).
[62]A. Zarembovitch, J. Phys. Radium 24, 1097 (1963); Bull. Soc. France Mineral. Crist. 88, 17 (1965).
[63]B. H. Lee, J. Appl. Phys. 41, 2984 (1970).
[64]D. Gerlich, J. Phys. Chem. Solids 28, 2575 (1967).
[65]Yu. Kh. Vekilov and A. P. Rusakov, Fiz. Tverd. Tela 13, 1157 (1971) [Sov. Phys. Solid State 13, 956 (1971)].
[66]A. Lehoczky, Bull. Am. Phys. Soc. 14, 393 (1969).
[67]T. Alper and G. A. Saunders, J. Phys. Chem. Solids 28, 1637 (1967).
[68]P. Flubacher, A. J. Leadbetter, and J. A. Morrison, Phil. Mag. 4, 273 (1959).
[69]C. W. Garland and K. C. Park, J. Appl. Phys. 33, 759 (1962).
[70]C. T. Cetas, C. R. Tilford, and C. A. Swenson, Phys. Rev. 174, 835 (1968).
[71]L. J. Slutsky and C. W. Garland, Phys. Rev. 113, 167 (1959).
[72]C. J. Glassbrenner and G. A. Slack, Phys. Rev. 134, A1058 (1964).
[73]R. O. Carlson, G. A. Slack, and S. J. Silverman, J. Appl. Phys. 36, 505 (1965).
[74]G. Busch and E. Steigmeier, Helv. Phys. Acta 34, 1 (1961).
[75]J. G. Mavroides and D. F. Kolesar, Solid State Commun. 2, 363 (1964).
[76]E. F. Steigmeier, Appl. Phys. Letters 3, 6 (1963).
[77]J. T. Vallin, G. A. Slack, S. Roberts, and A. E. Hughes, Phys. Rev. B 2, 4313 (1970).
[78]G. Herzberg, *Infrared and Raman Spectra* (Van Nostrand, Princeton, 1945), p. 100.
[79]G. F. Koster, J. O. Dimmock, R. G. Wheeler, and H. Statz, *Properties of the Thirty-Two Point Groups* (M. I. T. Press, Cambridge, Mass., 1963).

PHYSICAL REVIEW B VOLUME 6, NUMBER 10 15 NOVEMBER 1972

Frequency- and Wave-Vector-Dependent Dielectric Function for Ge, GaAs, and ZnSe †

S. J. Sramek and Marvin L. Cohen
Department of Physics, University of California, Berkeley, California 94720
and Inorganic Materials Research Division, Lawrence Berkeley Laboratory, Berkeley, California 94720
(Received 30 June 1972)

The frequency- and wave-vector-dependent dielectric function for Ge, GaAs, and ZnSe is calculated from the electronic band structures obtained by the empirical-pseudopotential method. The results show the effect of increasing ionicity on the dielectric function. The results also yield the plasmon dispersion relation $\omega(q)$ for the three semiconductors. The frequency- and wave-vector-dependent Penn dielectric function is calculated and compared with the results for Ge.

I. INTRODUCTION

We have calculated[1] the frequency- and wave-vector-dependent dielectric function $\epsilon(\vec{q}, \omega)$ in the [100] direction for Ge, GaAs, and ZnSe. This dielectric function describes the screening of a longitudinal field which varies in both space and time. This is the first calculation of $\epsilon(\vec{q}, \omega)$ for these materials using realistic energy bands and wave functions. These three crystals were chosen to observe the changes in $\epsilon(\vec{q}, \omega)$ as one moves through a series from a completely covalent compound (Ge) to compounds with decreasing covalency (GaAs and ZnSe).

The present calculations of $\epsilon(\vec{q}, \omega)$ are similar to that done by Walter and Cohen[2] for Si. The real part of the dielectric function, $\epsilon_1(\vec{q}, \omega)$, is calculated directly, and the imaginary part, $\epsilon_2(\vec{q}, \omega)$, is calculated using the Kramers–Kronig transformation. The details and results of the calculation are given in Sec. II. In Sec. III the results for Ge are compared with a calculation of $\epsilon_1(\vec{q}, \omega)$ using the Penn model.[3]

II. CALCULATIONS AND RESULTS

First we calculate the longitudinal-wave-vector- and frequency-dependent dielectric function $\epsilon(\vec{q}, \omega)$ which describes the crystal response to an electric field parallel to $\vec{q}$ and varying sinusoidally in time:

$$\vec{D}e^{i(\vec{q}\cdot\vec{r}-\omega t)} = \epsilon(\vec{q}, \omega)\vec{E}e^{i(\vec{q}\cdot\vec{r}-\omega t)}. \tag{2.1}$$

Using the result for ϵ_1 obtained by Ehrenreich and Cohen,[4] we obtain

$$\epsilon_1(\vec{q}, \omega) = 1 + \frac{4\pi e^2}{\Omega q^2} \sum_{\vec{k}, c, v} |\langle \vec{k}, c | \vec{k}+\vec{q}, v \rangle|^2 \times \{[E_c(\vec{k}) - E_v(\vec{k}+\vec{q}) - \hbar\omega]^{-1}$$

$$+[E_c(\vec{k})-E_v(\vec{k}+\vec{q})+\hbar\omega]^{-1}\}. \quad (2.2)$$

The matrix element is the inner product between the periodic parts of the Bloch functions, $\vec{k}$ is summed over the first Brillouin zone, v labels the valence bands, and c labels the conduction bands. For computational purposes Eq. (2.2) is rewritten as

$$\epsilon_1(\vec{q},\omega)=1+\frac{4\pi e^2}{q^2}\frac{2}{(2\pi)^3}\sum_{\vec{k},c,v}|\langle\vec{k},c|\vec{k}+\vec{q},v\rangle|^2(\Delta k)^3 \times\{[E_c(\vec{k})-E_v(\vec{k}+\vec{q})-\hbar\omega]^{-1} +[E_c(\vec{k})-E_v(\vec{k}+\vec{q})+\hbar\omega]^{-1}\}, \quad (2.3)$$

where the summation is over a grid of 3360 points in the Brillouin zone. $(\Delta k)^3$ is the volume of a cube associated with each point, with suitable truncations at the zone boundaries. The coordinates of the calculated points are given by $\frac{1}{16}(2s+1, 2m+1, 2n+1)$ in units of $2\pi/a$, where s, m, and n are integers. The indices v and c span the top four valence bands and the bottom 11 conduction bands. The wave functions and energies are obtained by the empirical-pseudopotential method,[5] using the pseudopotential form factors of Cohen and Bergstresser.[6] Spin-orbit interactions were not included in this calculation.

The dielectric function cannot be calculated for an arbitrary $\vec{q}$ because of computer time limitations. Crystal symmetry can be exploited to reduce considerably the time if $\vec{q}$ is restricted to the [100] direction. In addition, $|\vec{q}|$ must be restricted to the values $\frac{1}{8}n$, in units of $2\pi/a$, where n is an integer, so that $\vec{k}+\vec{q}$ also lies on the grid of calculated points.

The term $[E_c(\vec{k})-E_v(\vec{k}+\vec{q})-\hbar\omega]^{-1}$ in Eq. (2.3) can have singularities at some points in the Brillouin zone. If the cube of volume $(\Delta k)^3$ contains such points, then the energy values at the cube center cannot accurately represent $(E_c-E_v-\hbar\omega)^{-1}$ over the entire cube. For such cases, the large cube is divided into 216 equal subcubes, and the energies E_c and E_v are calculated for each subcube by interpolation.

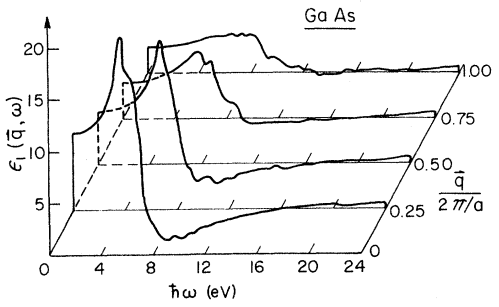

FIG. 2. $\epsilon_1(\vec{q},\omega)$ for GaAs.

After calculating $\epsilon_1(\vec{q},\omega)$, we calculate the imaginary part $\epsilon_2(\vec{q},\omega)$ by a Kramers–Kronig transform of $\epsilon_1(\vec{q},\omega)$. Figures 1–6 display three-dimensional perspective plots of $\epsilon_1(\vec{q},\omega)$ and $\epsilon_2(\vec{q},\omega)$ for the three semiconductors. Each curve represents ϵ_1 or ϵ_2 as a function of ω for fixed $\vec{q}$. The q values are $q=\frac{1}{4}, \frac{1}{2}, \frac{3}{4}$, and 1 in units of $2\pi/a$ in the [100] direction. The dielectric functions were also calculated for $q=\frac{1}{8}, \frac{3}{8}, 1\frac{1}{4}, 1\frac{1}{2}$, and 2, but those results are not plotted.

By considering the points $(\vec{q},\omega)$ for which the calculated $\epsilon_1=0$, and by fitting a curve through these points, we obtain for each material two curves in the $(\vec{q},\omega)$ plane along which $\epsilon_1(\vec{q},\omega)=0$, which we denote by $\omega_t(q)$ and $\omega_l(q)$. The results are plotted in Fig. 7. From Eq. (2.1) we see that, if $\epsilon(\vec{q},\omega)=0$, then a nonzero electric field can exist in the material even if no field is applied externally; i.e., a plasmon can be present. For the three materials considered here, the lower zero $\omega_t(q)$ does not represent a physically observable plasmon mode, because (as can be seen in Figs. 1–6) both ϵ_1 and ϵ_2 are always near their largest values when near $\omega_t(q)$; i.e., $\omega_t(q)$ resembles a damped pole in ϵ_1.

As we move through the series from completely covalent Ge through somewhat ionic GaAs to the higher ionicity compound ZnSe, we observe three important qualitative features of ϵ_1: (a) The higher zeros of ϵ_1, representing the plasmon mode

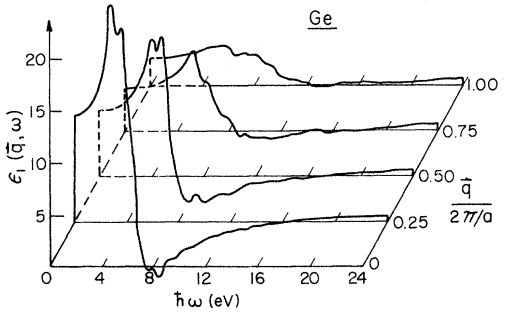

FIG. 1. $\epsilon_1(\vec{q},\omega)$ for Ge.

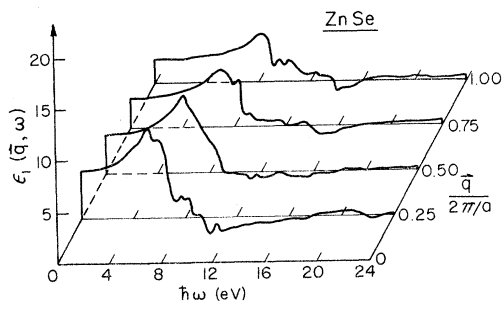

FIG. 3. $\epsilon_1(\vec{q},\omega)$ for ZnSe.

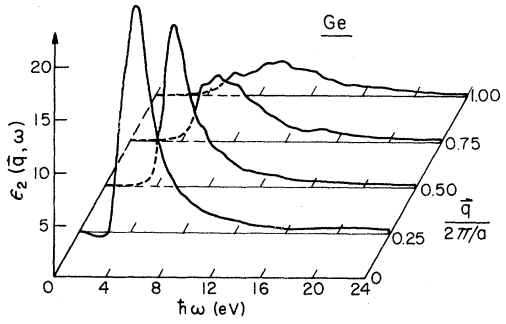

FIG. 4. $\epsilon_2(\vec{q},\omega)$ for Ge.

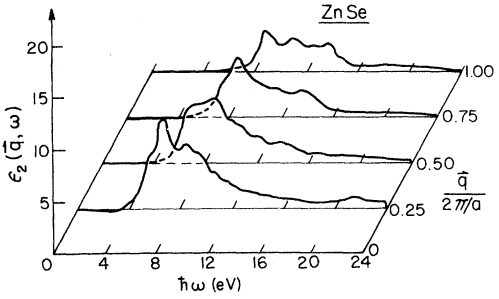

FIG. 6. $\epsilon_2(\vec{q},\omega)$ for ZnSe.

$\omega_t(q)$, change very little; (b) the lower zeros of ϵ_1, $\omega_t(q)$, increase substantially; and (c) the $\omega = 0$ values and the peak values of ϵ_1 decrease substantially. The reasons for these effects may be understood by examining Eq. (2.2).

Because Ge, GaAs, and ZnSe all have almost exactly the same lattice constant and are composed of elements all from the same row of the Periodic Table, they all have almost exactly the same symmetric pseudopotential. The principal change in moving through the series is that an antisymmetric psuedopotential is introduced and becomes larger. For a given $(\vec{k},c,v)$ the energy difference $E_c(\vec{k}) - E_v(\vec{k}+\vec{q})$ tends to become *larger*. Assuming that changes in the matrix elements in Eq. (2.2) are not important, we may conclude the following.

(i) At high frequencies, $\hbar\omega \gg E_c - E_v$ for all band pairs (c,v) for which the matrix elements are not small. Then

$$(E_c - E_v - \hbar\omega)^{-1} + (E_c - E_v + \hbar\omega)^{-1} \to 2(E_c - E_v)/(\hbar\omega)^2 ,$$

and we expect $\epsilon_1(q,\omega)$ at high frequencies to be only weakly dependent on the energy differences $E_c - E_v$. The true plasmon mode $\omega_t(q)$ should therefore be little affected by the antisymmetric pseudopotential and in fact is not far from the free-electron value (e.g., 15.6 eV for Ge).

(ii) For small frequencies, $\hbar\omega < E_c - E_v$ for all $(\vec{k}, c, v)$; as $\hbar\omega$ increases, $(E_c - E_v - \hbar\omega)^{-1}$ at first increases rapidly so that all terms in the sum over $(\vec{k},c,v)$ increases rapidly. $\epsilon_1(\vec{q},\omega)$ reaches a peak and begins decreasing when $\hbar\omega$ *passes* the smallest of the energy differences $E_c - E_v$, so that some of the terms $(E_c - E_v - \hbar\omega)^{-1}$ suddenly become large and *negative*. $\epsilon_1(\vec{q},\omega)$ passes through zero when so many of the terms $(E_c - E_v - \hbar\omega)^{-1}$ have become negative that they balance the positive terms in the sum over $(\vec{k},c,v)$. This occurs when $\hbar\omega$ becomes roughly equal to an "average energy gap" between the top valence and the bottom conduction bands. This value is probably connected with the Phillips average gap.[7] When the antisymmetric pseudopotential is introduced and the energy differences $E_c - E_v$ become larger, the frequency $\hbar\omega$ at which the negative terms $(E_c - E_v - \hbar\omega)^{-1}$ balance the positive terms in the sum over $(\vec{k},c,v)$ must also become larger. The lower zero $\omega_t(q)$ should therefore increase.

(iii) At zero frequency, Eq. (2.2) becomes

$$\epsilon_1(q,\omega=0) = 1 + \frac{8\pi e^2}{\Omega q^2} \sum_{\vec{k},c,v} |\langle \vec{k}, c | \langle \vec{k}+\vec{q}, v \rangle|^2$$

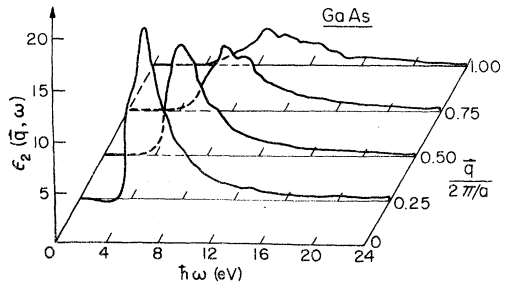

FIG. 5. $\epsilon_2(\vec{q},\omega)$ for GaAs.

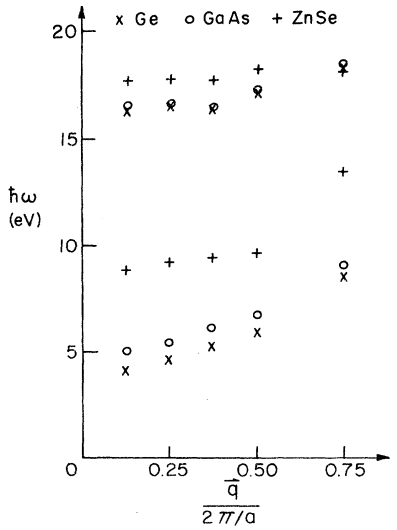

FIG. 7. Zeros of $\epsilon_1(\vec{q},\omega)$ for Ge, GaAs, and ZnSe.

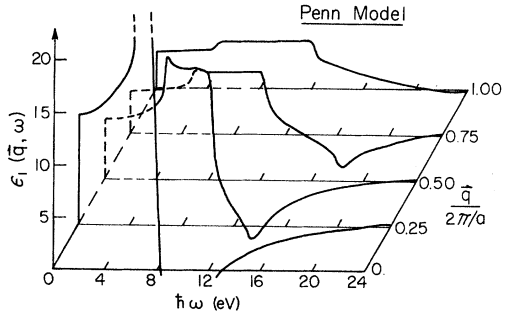

FIG. 8. $\epsilon_1(\vec{q},\omega)$ for the Penn model.

$$\times[E_c(\vec{k})-E_v(\vec{k}+\vec{q})]^{-1}.$$

Since the antisymmetric pseudopotential causes the energy differences E_c-E_v to increase, all terms in the sum decrease. The static and low-frequency values of ϵ_1 should therefore decrease.

III. PENN MODEL

We have calculated the Penn-model dielectric function for comparison with our Ge results. This model makes the following assumptions: (1) There is no Brillouin zone; (2) the energy $E(\vec{k})$ is spherically symmetric, with a step discontinuity of magnitude E_g at the Fermi surface; and (3) the eigenfunction of wave vector $\vec{k}$ is a superposition of just two plane waves, of wave vectors $\vec{k}$ and $\vec{k}-2k_F\hat{k}$. Using these assumptions, one can set up and solve a simple 2×2 secular equation and obtain analytic expressions for $E(\vec{k})$ and for the eigenfunctions. These expressions are given by Penn.[3] The dielectric function of this electron gas can then be calculated as a sum similar to (2.2).

In previous zero-frequency calculations,[3,8] to avoid the use of computing machines, Penn's expressions for $E(\vec{k})$ and for the matrix elements in (2.2) were replaced with simplified expressions. In particular, $E(\vec{k})$ was assumed to be parabolic (i.e., free-electron-like) everywhere except in a region near the Fermi surface; there, $E(\vec{k})$ is assumed equal to $E_F\pm\frac{1}{2}E_g$ (+ for $k>k_F$, − for $k<k_F$), so that the "bands" are perfectly flat in a region near the Fermi surface, with an energy gap E_g.

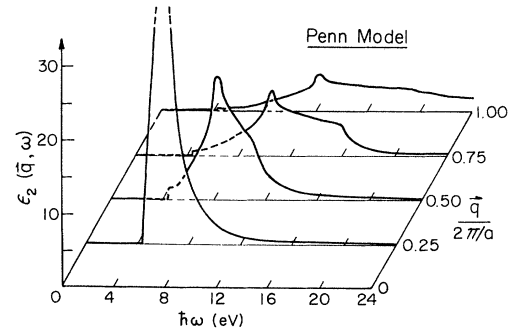

FIG. 9. $\epsilon_2(\vec{q},\omega)$ for the Penn model.

TABLE I. Comparison of the Penn-model $\epsilon_1(\vec{q},\ \omega=0)$ with the result of Walter and Cohen.

q $(2\pi/a)$	$\epsilon_1(\vec{q},\ \omega=0)$ Walter and Cohen	Penn model
0.125	12.7	14.8
0.250	10.3	10.5
0.375	8.0	7.5
0.500	6.2	5.7
0.750	4.0	4.0
1.000	2.8	3.5

One can easily show that this "flat-band" simplification will cause $\epsilon_1(\vec{q},\omega)$ to exhibit a first-order pole *exactly* at $\hbar\omega=E_g$ for all $q<2k_F$. Because the lower zero of the Ge $\epsilon_1(\vec{q},\omega)$ increases significantly with $\vec{q}$ (Fig. 7), we expect that the Penn model with the flat-band simplification cannot closely approximate the calculated $\epsilon_1(\vec{q},\omega)$ for Ge.

Accordingly, we have numerically computed the Penn dielectric function using the exact $E(\vec{k})$ and eigenfunctions proposed by Penn. We chose $E_g=4.3$ eV, the principal optical gap of Ge, and k_F so that the associated electron concentration is equal to the Ge valence-electron concentration. The results are plotted in Figs. 8 and 9.

The Penn model $\epsilon_1(\vec{q},\omega=0)$ agrees fairly well with the result of Walter and Cohen[9] (identical to our result) for Ge. The numbers are given in Table I. However, for intermediate and high frequencies the agreement is poor. The Penn-model polarizability at higher frequencies is considerably larger than the calculated Ge polarizability based on the Ge $E(\vec{k})$. As a result, the upper zeros of $\epsilon_1(\vec{q},\omega)$ occur at appreciably higher frequencies than in the Ge case.

This low-frequency agreement and high-frequency disagreement may be understood as follows: The dielectric function for zero frequency is of the form

$$\epsilon_1(\vec{q},\omega=0)=1+\frac{1}{q^2}\sum\frac{M^2}{E_{\vec{k}+\vec{q}}-E_{\vec{k}}}\ ,$$

whereas for high frequencies

$$\epsilon_1(\vec{q},\omega\to\infty)=1-\frac{1}{(\hbar\omega)^2}\frac{1}{q^2}\sum M^2(E_{\vec{k}+\vec{q}}-E_{\vec{k}})\ .$$

So, for low frequencies the polarizability involves the ratios of matrix elements and energy differences, whereas for high frequencies it involves the products of matrix elements and energy differences. We suggest that both the energy differences $E_{\vec{k}+\vec{q}}-E_{\vec{k}}$ and the valence-conduction coupling matrix elements M^2 tend to be larger for the Penn model than

for true Ge. If so, then the high-frequency Penn-model polarizability, involving the products $M^2(E_{\vec{k}+\vec{q}} - E_{\vec{k}})$, should be considerably larger than the values for Ge, whereas the low-frequency polarizability, involving the ratios $M^2/(E_{\vec{k}+\vec{q}} - E_{\vec{k}})$, may not be substantially different from the Ge case.

ACKNOWLEDGMENT

We would like to thank Professor John Walter for his help with the computer programming.

†Research supported in part by the National Science Foundation, under Grant No. GP 13632. Work done under the auspices of the U. S. AEC.

[1]A preliminary account of the results of the present work was given by S. J. Sramek and M. L. Cohen, Bull. Am. Phys. Soc. 17, 26 (1972).

[2]John Walter and M. L. Cohen, Phys. Rev. B 5, 3101 (1972).

[3]D. R. Penn, Phys. Rev. 128, 2093 (1962).

[4]H. Ehrenreich and M. H. Cohen, Phys. Rev. 115, 786 (1959).

[5]M. L. Cohen and V. Heine, Solid State Phys. 24, 37 (1971).

[6]M. L. Cohen and T. K. Bergstresser, Phys. Rev. 141, 789 (1966).

[7]J. C. Phillips, Rev. Mod. Phys. 42, 317 (1970).

[8]G. Srinivasan, Phys. Rev. 178, 1244 (1969).

[9]John Walter and M. L. Cohen, Phys. Rev. B 2, 1821 (1970).

PHYSICAL REVIEW B VOLUME 6, NUMBER 10 15 NOVEMBER 1972

Infrared Absorption by Coupled Surface-Phonon–Surface-Plasmon Modes in Microcrystals of CdO

K. H. Rieder, M. Ishigame,* and L. Genzel
Max-Planck-Institut für Festkörperforschung, Stuttgart, Germany
(Received 23 June 1972)

The first observation of surface-phonon–surface-plasmon coupling in small particles is reported. Thin layers of semiconducting CdO microcrystals with various free-carrier concentrations were used as samples. The coupling manifests itself in the infrared-absorption spectra through two absorption maxima corresponding to two resonances of the coupled two-oscillator system and through a pronounced absorption minimum near the transverse-optical-phonon frequency ω_T. The experimental results are discussed on the basis of a theoretical approach recently developed by Genzel and Martin. Structure in the absorption spectra near the longitudinal-optical-phonon frequency ω_L is attributed to the strong polar-optical scattering of free carriers in CdO.

I. INTRODUCTION

The phenomenon of surface-plasmon–surface-phonon coupling has met considerable theoretical interest. According to the mathematical accessibility, the problem has been studied for two situations: First, the case of infinitely extended surfaces bounding a half-space of a polar dielectric[1-3] and second, the case of small crystalline particles of certain shapes.[4,5] Both cases are amenable to experimental investigations. Plasmons and phonons at extended surfaces can be studied by the prism-coupling method proposed by Otto[6] and used already by Marschall *et al.*[7] in studying the dispersion of surface plasmons as well as by Marschall and Fischer[8] and also by Bryksin *et al.*[8] in investigating surface phonons. Using the prism-coupling technique, Reshina *et al.*[9] have observed very recently coupled surface-phonon–surface-plasmon modes at extended surfaces of *n*-type InSb. Surface phonons in small ionic crystals have been studied extensively in the last years by infrared-absorption measurements.[10-15] Also, surface plasmons in small metallic particles have been detected by optical methods.[16-18] The present paper deals with the first investigation of a coupled system of surface phonons and surface plasmons in microcrystals of an ionic semiconductor by means of infrared absorption.

For an understanding of the experimental results, Sec. II gives a concise account of the theoretical approach of Genzel and Martin.[5] Section III is devoted to a description of the experimental procedure. In Sec. IV, the experimental infrared-absorption curves are discussed on the basis of the theory.

II. THEORETICAL SURVEY

Genzel and Martin[5,11] have developed a continuum model appropriate for describing the dielectric properties of spheres with sizes very much smaller than the wavelength of the electromagnetic radiation. They consider a medium composed of separated particles with bulk dielectric function $\epsilon(\omega)$